

# Study of Low-Energy Fission Actinide-Nuclei with Fourier Shape Parametrization

**P.V. Kostryukov, A. Dobrowolski**

Theoretical Physics Department, Maria Curie-Skłodowska University,  
20-031 Lublin, Poland

**Abstract.** In present work the calculations of characteristics of the low-energy binary fission of actinide nuclei were presented. These values were obtained in the framework of Langevin equation formalism, where quantities related with nuclear surface were performed within Fourier shape parametrization. Using of global deformation parameters approach for obtaining of the excitation energies formed fission fragments at the neck breaking moment were performed. Making an assumption that cooling of primary fragments passes via neutron evaporation helped to build the secondary fragments mass yields. Comparative analysis of mass distributions for neutron induced and spontaneous fission nuclei with  $Z$  in region 92–98 showed good agreement with analogous experimental data.

## 1 Introduction

Despite the long history since the discovery of nuclear fission process, the problems associated with its proper description still remain unsolved. This work is mostly focused on reproducing the fission dynamics of heavy nuclei with obtaining quantitative characteristics of phenomena, such as mass, charge and kinetic energy distributions (yields) of fragments (FMD, FCD and TKE correspondently). A starting point of our calculations relies on determining the potential energy surface falling from the last saddle point up to the scission configurations using the framework of the well-known macroscopic-microscopic approach. For the evolution of the nuclear surface along nuclear way to fission one decompose its shape into the Fourier series where the linear combination parameters of the sine and cosine functions are treated, in general, as deformation parameters. The stochastic formalism of multidimensional Langevin equations allows to generate a series of possible trajectories of a nucleus toward fission. In addition, taken into account temperature effects allow to describe fission events with different excitation energy. Eventually, the model has the possibility to determine the characteristics related to evaporation of light particles from already formed fission fragments. This model has been tested to describe the fission of the compound nucleus  $^{236}\text{U}$  and later on, extended to a set of even-even actinide nuclei.

## 2 Methods and Description

In this section it will be discussed the way of constructing of the statistical model of the fission process, where one discusses the way of walking on the multi-dimensional potential energy surface (PES) obeying classical laws of motion, which will be discussed in more details in the following. First of all, let us define the mentioned potential energy  $E_{\text{coll}}$  of a nucleus using well known since a few decades macroscopic-microscopic model:

$$E_{\text{coll}} = E_{\text{macro}} + E_{\text{micro}} = E_{\text{LSD}} + E_{\text{shell}} + E_{\text{pair}}, \quad (1)$$

where  $E_{\text{macro}}$  is calculated in the framework of the liquid drop model, in our case the Lublin-Strasbourg Drop (LSD) [1] which effectively reproduces experimental masses and fission barrier heights throughout the periodic table. The microscopic part  $E_{\text{micro}}$  describes the shell and pairing interaction effects. The shell correction  $E_{\text{shell}}$  is obtained by subtracting the average energy  $\tilde{E}$  from the sum of the single-particle (s.p.) energies  $e_k$  of occupied orbitals which are the eigenvalues of the mean-field Hamiltonian of the Yukawa-folded type [2]

$$E_{\text{shell}} = \sum_k e_k - \tilde{E}. \quad (2)$$

The average energy is evaluated using the Strutinsky prescription of averaging a discrete spectrum [3] with a 6th order correction polynomial. The pairing energy correction in turn is determined similarly as in (2) for shell effects

$$E_{\text{pair}} = E_{\text{BCS}} - \sum_k e_k - \tilde{E}_{\text{pair}} \quad (3)$$

except that the so-called average pairing term part of this interaction not taken into account [4] in the liquid drop smooth energy part.

### 2.1 Shape parametrization

For describing the PES function introduced in the preceding subsection it is necessary to know the surface geometry of the atomic nucleus. There are many types of nuclear shape parametrisations available in nuclear physics theory: Cassini ovaloids, spherical harmonics, Legendre polynomials, etc. However, in this work we will use quite recent so-called Fourier parametrization [5], which according to its name, represents nuclear shape in cylindrical coordinates  $(R, z, \varphi)$  through the Fourier series decomposition:

$$\rho_s^2(u, \mathbf{q}) = R_0^2 \sum_{n=1} \left[ a_{2n} \cos \left( \frac{2n-1}{2} \pi u \right) + a_{2n+1} \sin (n\pi u) \right], \quad (4)$$

where the parameter  $u = (z - z_{sh})/z_0$  is dimensionless coordinate which meaning is demonstrated in Figure 1,  $R_0 = 1.2A^{1/3}$  is the radius of spherical drop

and the Fourier coefficients  $a_i$  ( $i = 2, 3, \dots$ ) are related to the deformation parameters  $q_i$  through the following transformations:

$$q_2 = \frac{a_2^0}{a_2} - \frac{a_2}{a_2^0}; \quad q_3 = a_3; \quad q_4 = a_4 + \sqrt{(q_2/9)^2 + q_4^0{}^2}. \quad (5)$$

These coordinates are related with the shape elongation in  $R_0$  radius unit, left-right mass asymmetry of fission fragments, and the neck thickness. The remaining coordinates,  $a_{2n}$  or  $a_{2n+1}$ , due to their weak influence on the PES [5, 6], can be neglected in this work.

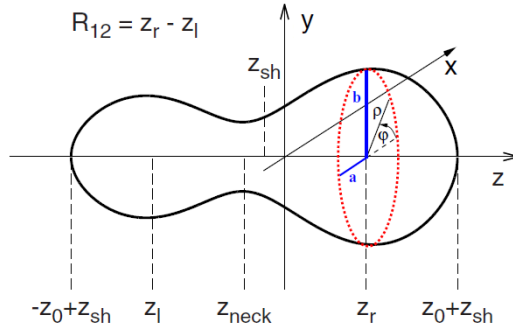


Figure 1. An example of nuclear body shape obtained [5] via Fourier parametrization.

Also, it should be noted that our collective deformation mesh grid on which all the above mentioned calculations have been performed can be characterized by the following boundaries and corresponding mesh node steps:

$$\begin{aligned} q_2 &= [-0.6 \ (0.05) \ 2.35] \\ q_3 &= [-0.21(0.03) \ 0.21] \\ q_4 &= [-0.21(0.03) \ 0.21] \end{aligned}$$

## 2.2 Shape evolution towards fission

In order to study the dynamics of fission of atomic nuclei, we use the formalism [7] of the multidimensional system of Langevin equations, which determines the the deformation of nuclear surface given in terms of generalized coordinates  $q_i$  (at this stage, they do not have to be identified with the above introduced Fourier shape parameters). Such equation system is similar to the canonical system of Hamilton equations if one neglects the collective friction and stochastic forces and can be represented as follows:

$$\begin{cases} \frac{dq_i}{dt} = \sum_j [\mathcal{M}^{-1}]_{ij} p_j, \\ \frac{dp_i}{dt} = -\frac{1}{2} \sum_{jk} \frac{\partial [\mathcal{M}^{-1}]_{jk}}{\partial q_i} p_j p_k - \sum_{jk} \gamma_{ij} [\mathcal{M}^{-1}]_{jk} p_k - \frac{\partial F}{\partial q_i} + \mathcal{R}_i, \end{cases} \quad (6)$$

where  $p_i$  is the conjugated momentum to the coordinate  $q_i$ ,  $\mathcal{M}_{ij}$  and  $\gamma_{ij}$  are inertia and friction tensors, respectively, while  $F$  is the Helmholtz free energy potentia of the compound fissile system

$$F(\mathbf{q}) = E_{\text{coll}}(\mathbf{q}) - a(\mathbf{q})T^2 = E_{\text{coll}}(\mathbf{q}) - E^*(\mathbf{q}). \quad (7)$$

Here  $a(\mathbf{q})$  is the density of energy levels of the compound nucleus determined as written in [8]. The last term in the second equation of the system (6),  $\mathcal{R}_i = \sum_j g_{ij} \Xi_j$ , is responsible for non-linearity,  $\Xi$  is the time-dependent function  $\Xi(t) = \xi/\sqrt{\tau}$  and the amplitude  $g_{ij}$  is related to the friction tensor and the temperature of the system  $T$  according [7] to the fluctuation-dissipation theorem known as the Einstein relation

$$\mathcal{D}_{ij} \equiv \sum_k g_{ik} g_{jk} = \gamma_{ij} T. \quad (8)$$

Note that the  $\xi$  function is defined as a random Gaussian distribution with white noise properties as  $\xi = 0$  and  $\xi^2 = 2$ .

The inertia (mass) tensor in (6) is calculated within the framework of the representation of the atomic nucleus as an incompressible and irrotational liquid, using the Werner-Wheeler approximation, presented in [9]

$$\mathcal{M}_{ij}(\mathbf{q}) = \pi \rho_m \int_{z_{\min}}^{z_{\max}} \rho_s^2(z, \mathbf{q}) \left[ A_i A_j + \frac{1}{8} \rho_s^2(z, \mathbf{q}) A'_i A'_j \right] dz, \quad (9)$$

where  $\rho_m = M_0/(\frac{4}{3}R_0^3)$  is the mass density, and the coefficients  $A_i$  have the form

$$A_i = \frac{1}{\rho_s^2(z, \mathbf{q})} \frac{\partial}{\partial q_i} \int_z^{z_{\max}} \rho_s^2(z', \mathbf{q}) dz'. \quad (10)$$

The coefficients  $A'_i$  in (9) are defined similar to (10) way by replacing the partial derivative operator of the coordinate  $q_i$  on  $z$ . Following the assumptions of [9], the authors of [10] continued to investigate viscosity properties of nuclear fluid and as a result obtained an expression defining the friction tensor  $\gamma_{ij}$  for one-body case by means of the so-called ‘‘wall’’ formula

$$\gamma_{ij}^{\text{wall}} = \frac{\pi}{2} \rho_m \bar{v} \int_{z_{\min}}^{z_{\max}} \frac{\partial \rho_s^2}{\partial q_i} \frac{\partial \rho_s^2}{\partial q_j} \left[ \rho_s^2 + \frac{1}{4} \left( \frac{\partial \rho_s^2}{\partial z} \right)^2 \right] dz, \quad (11)$$

where  $\bar{v}$  is the average internal velocity of nucleons in the nucleus, the value of which is related to the Fermi velocity  $v_F$  through  $\bar{v} = \frac{3}{4}v_F$ .

### 2.3 Boundary conditions

Before starting to calculate the Langevin trajectories, it is necessary to mention the importance of the boundary conditions. The careful choice of the starting point  $(q_2^{\text{start}}, q_3^{\text{start}}, q_4^{\text{start}})$  and the corresponding conjugated momenta seems to

be crucial. The starting configuration is chosen here as the one situated in the vicinity of the last saddle point before scission in the PES. It is clear that from there the system in question goes directly towards fission. In the case when the trajectory goes back, i.e. actual value of elongation  $q_2 < q_2^{\text{start}}$ , such a trajectory is considered as a non-physical one. So, for each trajectory at starting moment zero has the same position and energy. At the next point in time, new position is determined by using normal random function and amplitude determined by the stiffness of the potential in the saddle (however in the case of high values, it is limited by the distance between mesh nodes).

In this model we apply two major conditions for terminating of the nuclear shape evolution during calculation of each trajectory. The first is reaching a certain value of the neck radius  $R_{\text{neck}}$ , which is usually admitted to be close to 1.5 fm. The second is achieving the upper limit of the  $q_2$  coordinate, i.e.  $q_2 = 2.35$  since in this configuration the system breaks up anyway due to the domination of Coulomb interaction over the nuclear (surface term in the LSD formula) one. Note that in the case of reaching by a trajectory the limit at other than  $q_2$  coordinates, a kind of “wall reflection” procedure is used, i.e. one changes the sign of the corresponding conjugate momentum  $p$ .

### 3 Results and Discussion

One can demonstrate that the above developed model has the ability to reproduce in a reasonable way FMD's and TKE's for trajectory number being relatively small as for a stochastic approach. To get a satisfactory convergence in the reproduction of the above fission observables one typically simulates about  $N_{\text{traj}} = 5 \times 10^4$  events. Determination of the exit point of each trajectory gives unambiguously the fragmentation of a nucleus and kinetic energies of fission fragments in a single fission act. The full set of  $N_{\text{traj}}$  such single characteristics results with a distribution as the one presented on Figure 2.

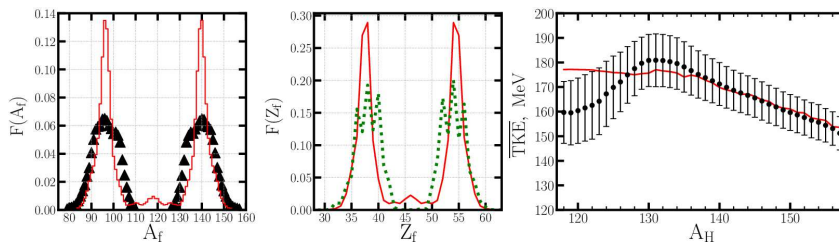


Figure 2. Primary FMD, FCD and  $\overline{\text{TKE}}$  of the neutron induced fission  $^{235}\text{U}$  (red curve),  $\blacktriangle$  and  $\bullet$  are analogous FMD and  $\overline{\text{TKE}}$  evaluated from experimental data [12] and [13].

### 3.1 Temperature dependences

From Figure 2 it can be seen that there is a significant difference between calculated and experimental data. This divergence can be attributed to the incomplete description of the presented “benchmark” as the temperature effects are not taken into account. First of all, it affects the microscopic energy term  $E_{\text{mic}}$  (2) of the collective potential (1). As the temperature rises the shell and pairing interaction are getting weaker and a nucleus becomes closer to a liquid drop. As shown in [8] this effect can be described on average by introducing a temperature-dependent multiplier in the form of a Fermi function of temperature as follows:

$$E_{\text{mic}}(\mathbf{q}, T) = c_{\text{temp}}(T)E_{\text{mic}}(\mathbf{q}, T = 0) = \frac{E_{\text{mic}}(\mathbf{q}, T = 0)}{1 + e^{(1.4-T)/0.25}}. \quad (12)$$

The results of the above modification is demonstrated in Figure 3, where one can observe the changes of the FMD with initial excitation energy, defining the initial temperature of the system.

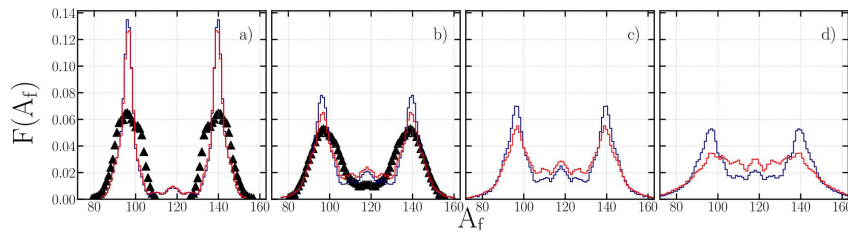


Figure 3. Primary FMD's for  $^{236}\text{U}$  obtained with excitation energies close to 6 MeV (a), 20 MeV (b), 35 MeV (c), 60 MeV (d) with (red) or without using (violet) coefficient (2).

Clearly, for low excitation energies, the shell effects remain predominant while the intrinsic friction force has than to stay small and starts growing with increasing temperature. According to the result presented in [14] we can, in addition, introduce a temperature-dependent coefficient for the friction tensor

$$\gamma_{ij}^{\text{mic}} = c_{\gamma}(T)\gamma_{ij}^{\text{wall}} = \frac{0.7\gamma_{ij}^{\text{wall}}}{1 + e^{(0.7-T)/0.25}}. \quad (13)$$

Comparing the results presented in Figure 4 one notice that the results of multiplication the friction tensor by temperature on constant values and temperature dependent factor (13) are noticeably different. Using the latter, one removes the appearance of events in symmetric fission channel, enchanting the symmetric one, which should not appear on thermal induced fission of  $^{235}\text{U}$ . Moreover, already for higher excitation energies around 20 MeV (see second row of Figure 4), the usage of  $c_{\gamma}(T)$  factor results with the closest to the available [13] experimental data. Note an interesting behaviour of the distribution (d)

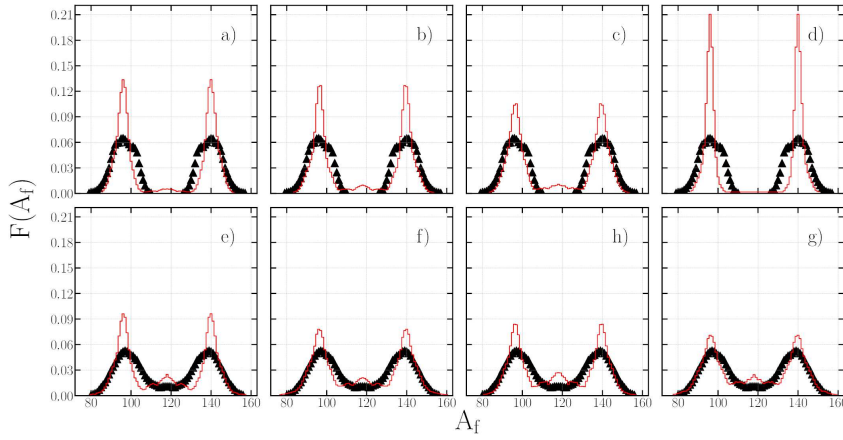


Figure 4. Primary FMD's for induced fission of  $^{235}\text{U}$  by thermal (a-d) and 14.8 MeV (e-g) neutrons, where friction tensors are multiplied by factors 0.5 (a, e), 1 (b, f), 2 (c, h) and temperature-dependent function  $c_\gamma(T)$  (d, g).

shown in Figure 5. At low excitation energy and hence temperature and diffusion tensor  $\mathcal{D}_{ij}$  (8), the surface configurations associated with symmetric fission practically disappear. However, the cost of this approach is the rapid decline in the region close to the symmetric fission region and formation of high peaks, which is not observed for the more excited states.

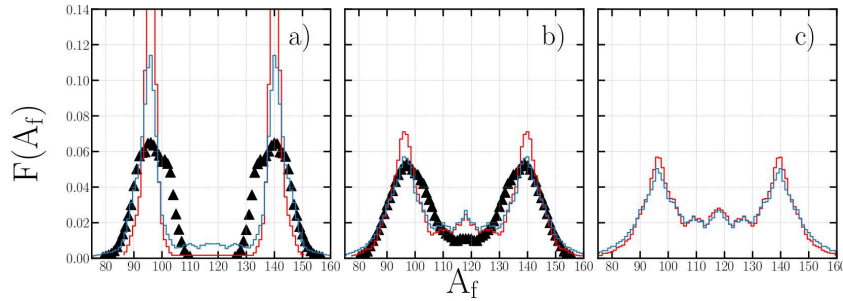


Figure 5. Comparison of primary FMD's with (blue line) and without (red line) usage of  $T^*$  for fission of compound nucleus  $^{236}\text{U}$  at 6(a), 20(b) and 35(c) MeV of excitation energy.

It is, however, necessary to realize that the notion of temperature in a classical sense does not fully apply in the quantum mechanical world, particularly when a system of finite number of a several tens to few hundred particles stays in its stable low-energy state, performing zero-point vibrations. This primarily indicates that the diffusion tensor (8), built on the basis of the principles of clas-

sical statistical physics has to be redefined so that the fact of the zero-point motion is, at least, effectively considered. It seems that the optimal solution of this problem is to redefine the temperature  $T$  onto effective temperature  $T^*$ , which, even in a cold nucleus has non-zero value, as it was introduced in [15]

$$T^* = E_0 \coth \frac{E_0}{T}, \quad (14)$$

where  $E_0$  corresponds to the zero-point collective vibrations energy of nucleons, which has value 1 MeV.

The use of the effective temperature (14) improves FMD and leads to a good agreement with corresponding experimental distributions. This was also tested not only on the well-studied isotope  $^{236}\text{U}$ , but also for several other nucleus-actinides undergoing induced or spontaneous fission. The results of the calculations for these isotopes are presented in Figure 6.

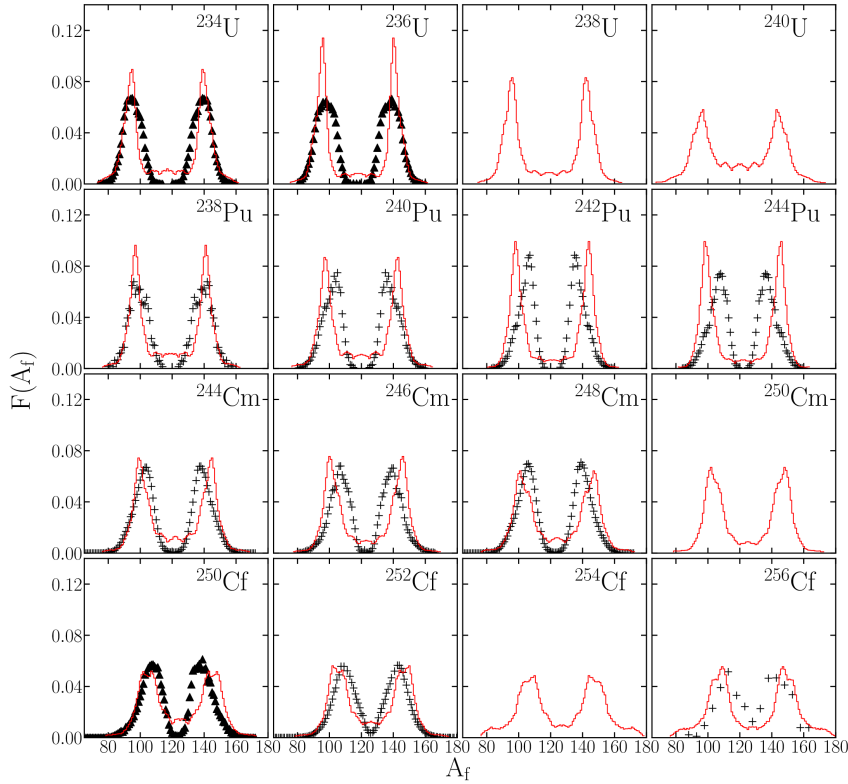


Figure 6. Primary FMD's for induced ( $\blacktriangle$ ) and spontaneous ( $+$ ) fission of nuclei-actinides taken from EXFOR database.

### 3.2 Particle emission

One has to notice that some FMD's in selected nuclei are measured after the emission of light particles, so they have to be compared with so called secondary FMD. To obtain such distributions, it is necessary to take into account the emission of light particles, e.g. neutrons, protons, and  $\alpha$ -particles from formed primary fission fragments. Within the low-energy fission process the overwhelming majority of particles emitted from fragments are neutrons for which the relaxation time of transition, according to the *Kramers formula* [7] can be taken to infinity. One can also assume that the energy released as a result rearrangement of the intrinsic structure of nucleus, it could be possible to postulate that temperature of the system upon breakup and already formed fragments are identical, i.e.  $E_f^* = a_f T^2$ . Another component of the excitation energy of fission fragments is the difference between the potential energy of the actual fragment deformation and its ground state, admitted in a first approximation as of spherical shape. These assumptions significantly simplify the calculation of secondary yields. Then the total excitation energy of fragment  $E_{\text{tot}f}^*$  with the absence of shell and pairing energy corrections can be written as

$$E_{\text{tot}f}^* = \Delta E_{\text{LSD}}(Z_f, A_f) + a_f T^2. \quad (15)$$

In that above, the deformations of both fragments were described using the so called *global deformation parameter*, introduced first in the work of Mayers and Swiatecki [17], where all surface coefficients of the liquid droplet model were represented through a series expansion of this single parameter. However, the accuracy of describing the potential energy within this method may not be satisfactory but for mentioned number trajectories it seems to be optimal.

With the above assumption, the maximum energy available for a neutron to be evaporated can be given as

$$\epsilon_n^{\text{max}} = M_{M_f} + E_{\text{tot}f}^* - M_{D_f} - M_n, \quad (16)$$

where symbols  $M$  denotes mass excesses of fragments of mother and daughter nuclei, respectively taken from tables whereas  $M_n$  is mass of a free neutron. If  $\epsilon_n^{\text{max}}$  has positive value the energy widths can be determined by the Weisskopf type formula [16]:

$$\Gamma_n(\epsilon_n^{\text{max}}) = \frac{2\mu}{(\pi\hbar)^2 \rho_M(E_M^*)} \int_0^{\epsilon_n^{\text{max}}} \sigma_{\text{inv}}(\epsilon) \epsilon_{QD}(E_D^*) d\epsilon. \quad (17)$$

In (17)  $\sigma_{\text{inv}}(\epsilon)$  is the inverse neutron cross section estimated within the phenomenological formula

$$\sigma_{\text{inv}}(\epsilon) = \pi \left(1.7A_f^{1/3}\right)^2 \left[0.76 + 1.93A_f^{-1/3} + \frac{1.66A_f^{-2/3} - 0.05}{\epsilon}\right] \quad (18)$$

and  $\varrho_i$  is the density of levels estimated in [8] through the expression

$$\varrho_M(E_f^*) = \frac{\sqrt{\pi} e^{2\sqrt{aE_f^*}}}{12 a^{1/4} E_f^{*5/4}}. \quad (19)$$

Determining the partial widths  $\Gamma_n$  and applying a Monte-Carlo type averaging, the energy  $\epsilon_n$  taken away by a neutron were calculated. Neutrons can potentially be evaporated until the residual energy  $\epsilon_{n+1}^{\max} = \epsilon_n^{\max} - \epsilon_n$  is positive. The results of above outlined calculations combined with the data shown on Figure 6 lead to the secondary FMD's, which are presented in Figure 7. An excellent similarity with experimental data can be noticed.

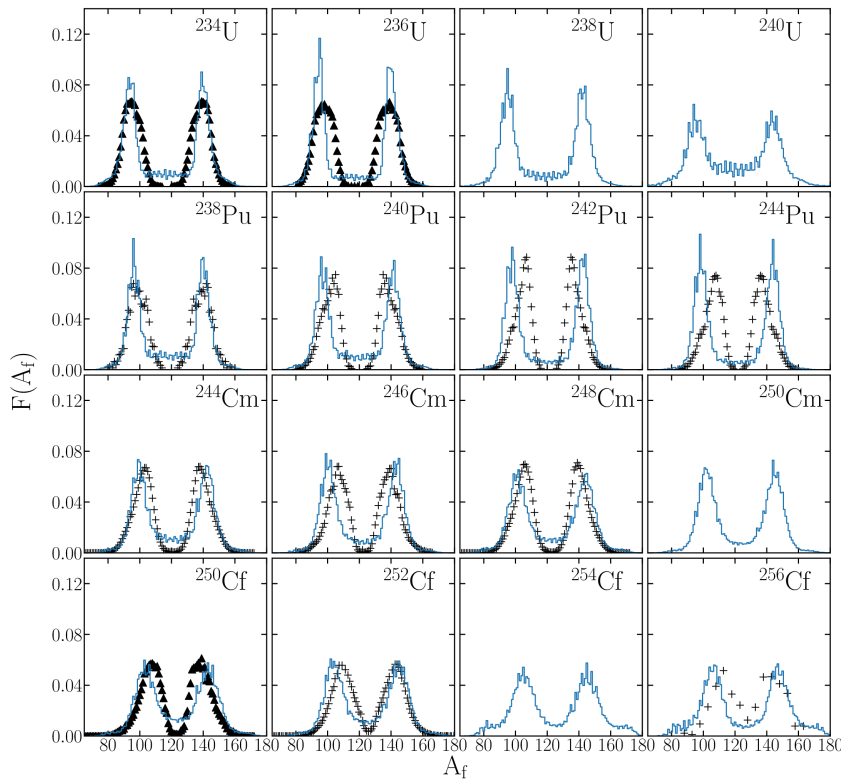


Figure 7. Secondary FMD's for induced (▲) and spontaneous (+) fission of nuclei-actinides .

#### 4 Conclusion

Within this work we demonstrate a power of the model for describing the low-energy fission of compound actinide nuclei based on the multidimensional sys-

tem of Langevin equations, where nuclear shapes are generated through a relatively new and well performed Fourier parametrization. The model is capable to determine mass, charge and kinetic energy distributions with or without temperature effects. The quality of obtained results is confirmed by reasonably good agreement of the primary FMD with experimental data. Taking into consideration the Master equation based on the Weisskopf formalism which describes the energies and emission probabilities of light particles (in particular, neutrons) allows us to approach closer to the experimental values.

### Acknowledgements

The authors are grateful to Prof. K. Pomorski for his support and fruitful discussions as well as to Prof. Y. J. Chen and Dr. L.L. Liu, collaborators of the Polish-Chinese SHENG program, for their useful comments and provided experimental data, which were very helpful during the writing of this paper. This international project was supported by the Polish National Science Center (Grant No 2018/30/Q/ST2/00185).

### References

- [1] K. Pomorski, J. Dudek, *Phys. Rev. C* **67** (2003) 044316.
- [2] A. Dobrowolski, K. Pomorski, J. Bartel, *Comp. Phys. Comm.* **118** (2016) 118.
- [3] V.M. Strutinsky, *Sov. J. Nucl. Phys.* **3** (1966) 449.
- [4] B. Nerlo-Pomorska, K. Pomorski, J. Bartel, *Int. J. Mod. Phys. E* **21** (2012) 1250050.
- [5] C. Schmitt, et al., *Phys. Rev. C* **95** (2017) 034612.
- [6] K. Pomorski, et al., *Chin. Phys. C* **45** (2021) 054109.
- [7] H.J. Krappe, K. Pomorski, *Theory of Nuclear Fission*, Lecture Notes in Physics (Springer-Verlag, Berlin, 2012).
- [8] B. Nerlo-Pomorska, K. Pomorski, J. Bartel, *Phys. Rev. C* **74** (2006) 034327.
- [9] K.T.R. Davies, A.J. Sierk, J.R. Nix, *Phys. Rev. C* **13** (1976) 2385.
- [10] J. Blocki, et al., *Ann. Phys.* **113** (1978) 330.
- [11] J. Bartel, et al., *Comp. Phys. Comm.* **249** (2019) 139.
- [12] G. Simon, et al., *Nucl. Instrum. Methods Phys. Res. A* **286** (1990) 220.
- [13] P.P. Dyachenko, B.D. Kuzminov, M.Z. Tarasko, *Sov. J. Nucl. Phys.* **8** (1969) 165.
- [14] F.A. Ivanyuk, K. Pomorski, *Phys. Rev. C* **53** (1996) 1861.
- [15] H. Hofmann, D. Kiderlen, *Int. J. Mod. Phys. E* **7** (1998) 243.
- [16] H. Delagrangé, et al., *Z. Phys. A* **323** (1986) 437.
- [17] W.D. Myers, W.J. Swiatecki, *Nucl. Phys.* **81** (1966) 1.